Supplemental Materials: Shortest-path percolation on scale-free networks

Minsuk Kim, Lorenzo Cirigliano, Claudio Castellano, Hanlin Sun, Robert Jankowski, Anna Poggialini, and Filippo Radicchi

SUPPLEMENTARY FIGURES

In this section, we provide detailed numerical results that are not displayed in the main paper.

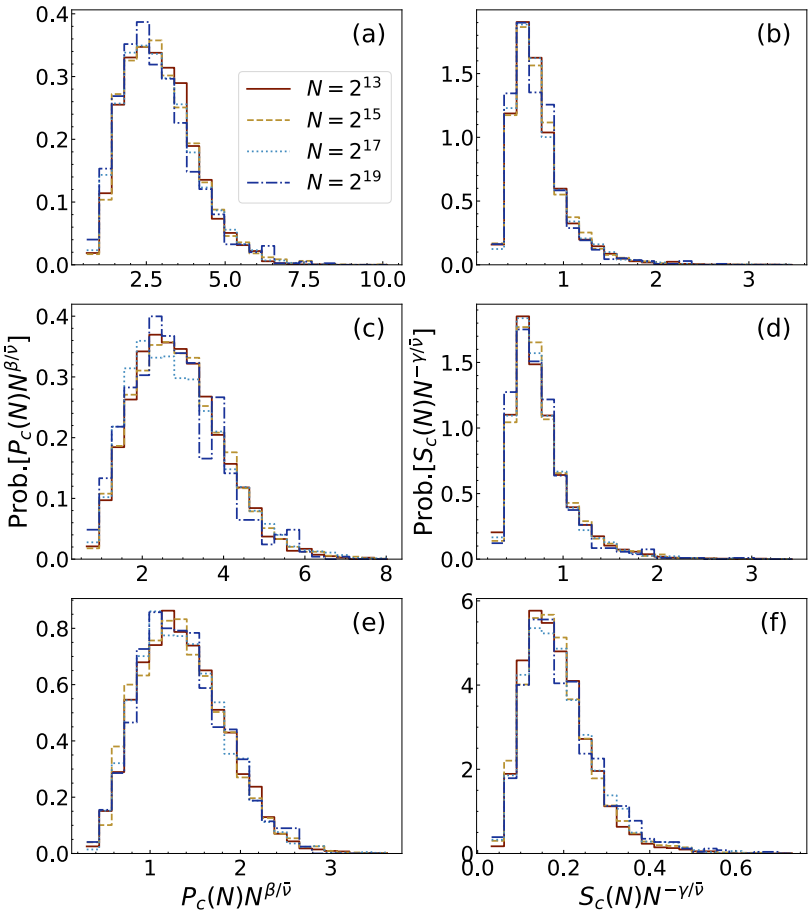

FIG. S1. **Data Collapse of probability distributions of critical observables.** Similar to Fig. 2 in the main, but results are valid for SFNs with $\lambda = 2.1$.

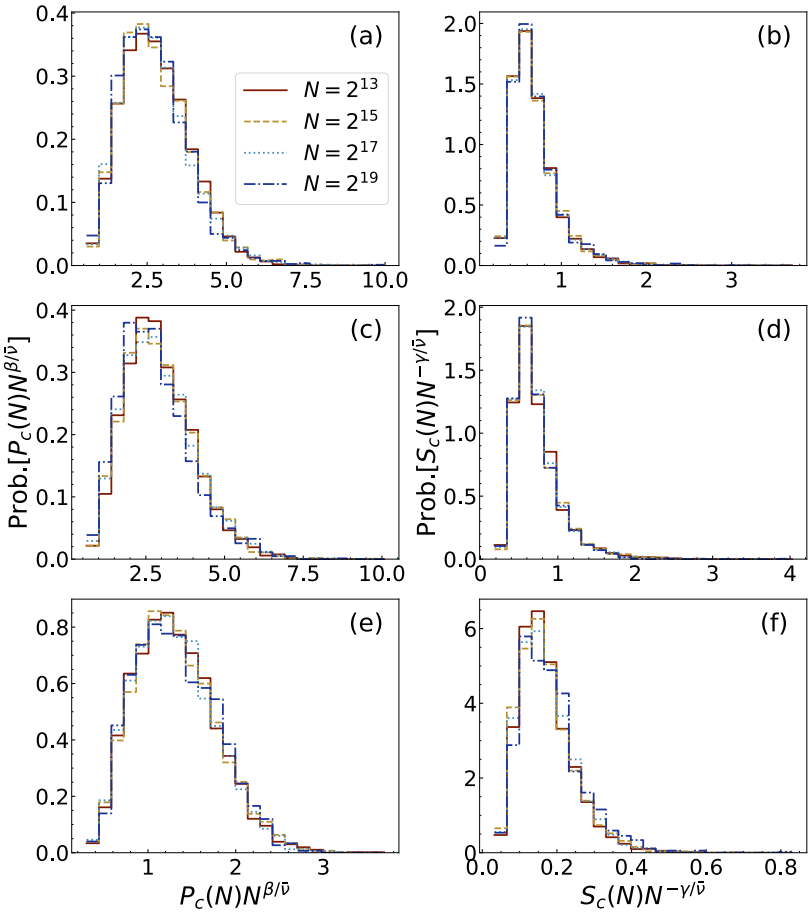

FIG. S2. **Data Collapse of probability distributions of critical observables.** Similar to Fig. 2 in the main, but results are valid for SFNs with $\lambda = 3.5$.

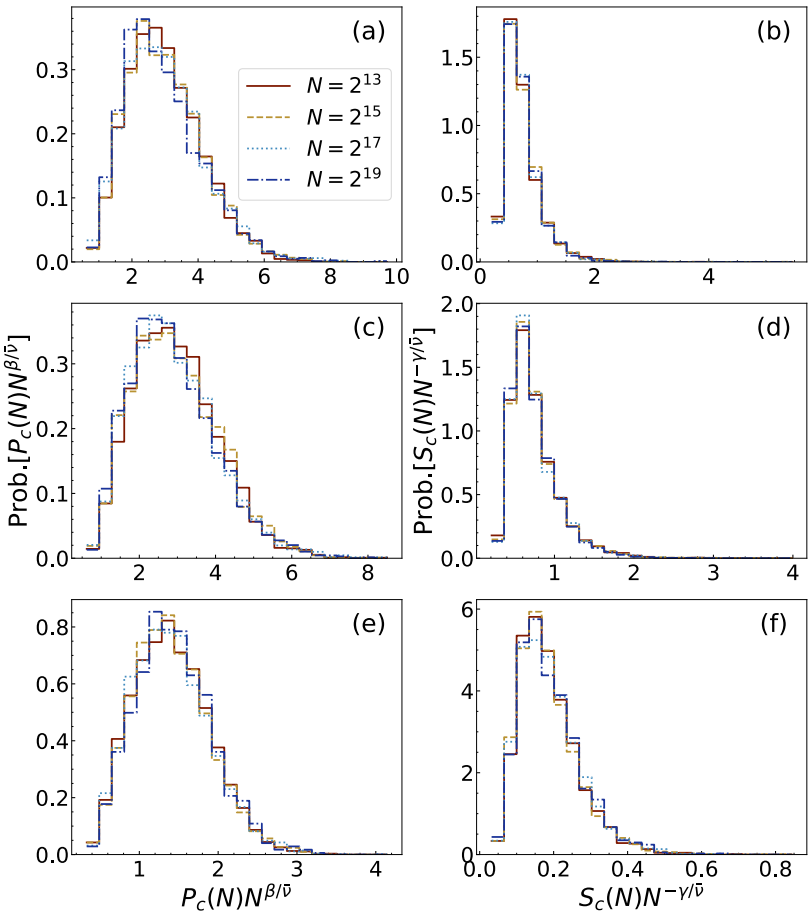

FIG. S3. **Data Collapse of probability distributions of critical observables.** Similar to Fig. 2 in the main, but results are valid for SFNs with $\lambda = 4.5$.

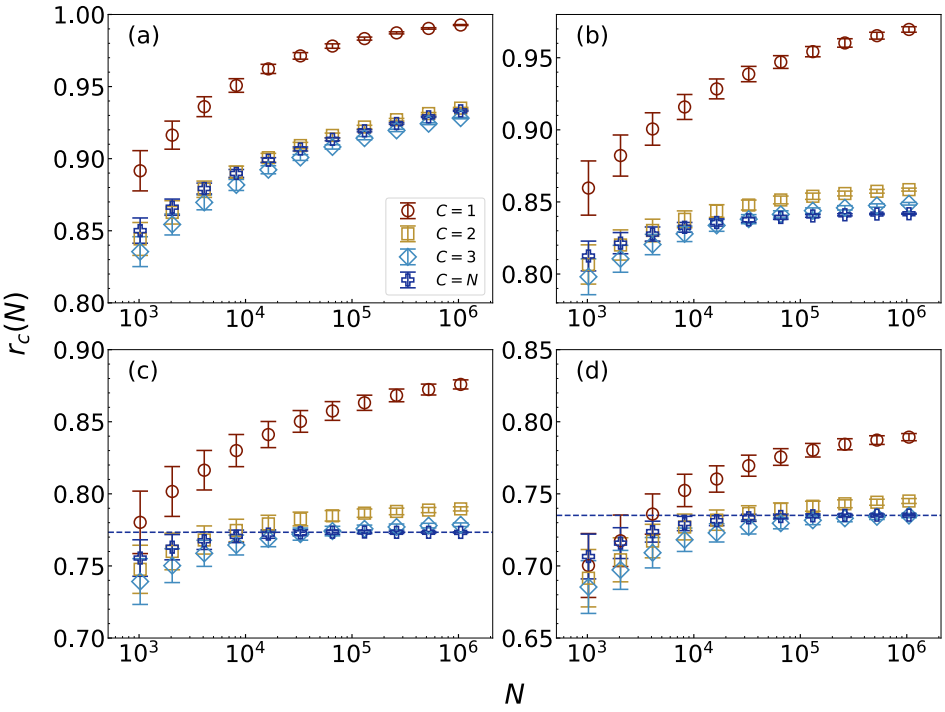

FIG. S4. **Pseudocritical point** $r_c(N)$. We plot the pseudocritical point $r_c(N)$ as a function of network size N. Results are valid for SFNs with (a) $\lambda = 2.1$, (b) $\lambda = 2.7$, (c) $\lambda = 3.5$, and (d) $\lambda = 4.5$. Note that the horizontal dashed lines in panel (c) and (d) are the plateau values of $r_c(N)$ for SPP with $C = N$. These values are obtained by taking the average of $r_c(N)$ with $N > 10^5$, which are within the error bounds reported in Table I.

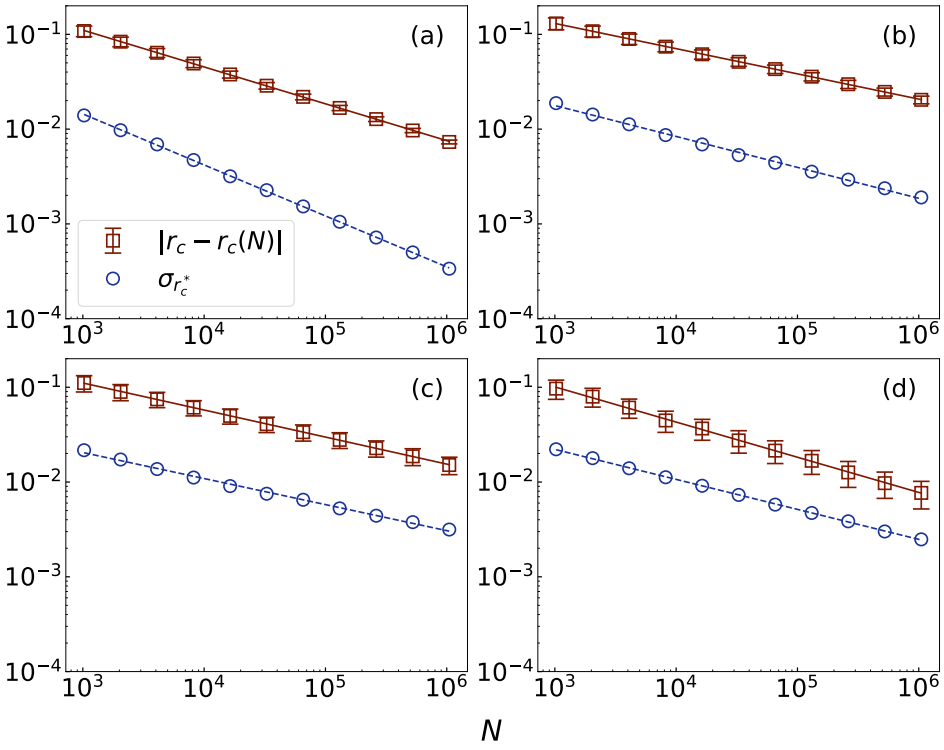

FIG. S5. **Estimation of $1/\bar{\nu}$.** Similar to Fig. 4 in the main, but results are valid for SPP with $C = 1$. Note that this corresponds to ordinary bond percolation.

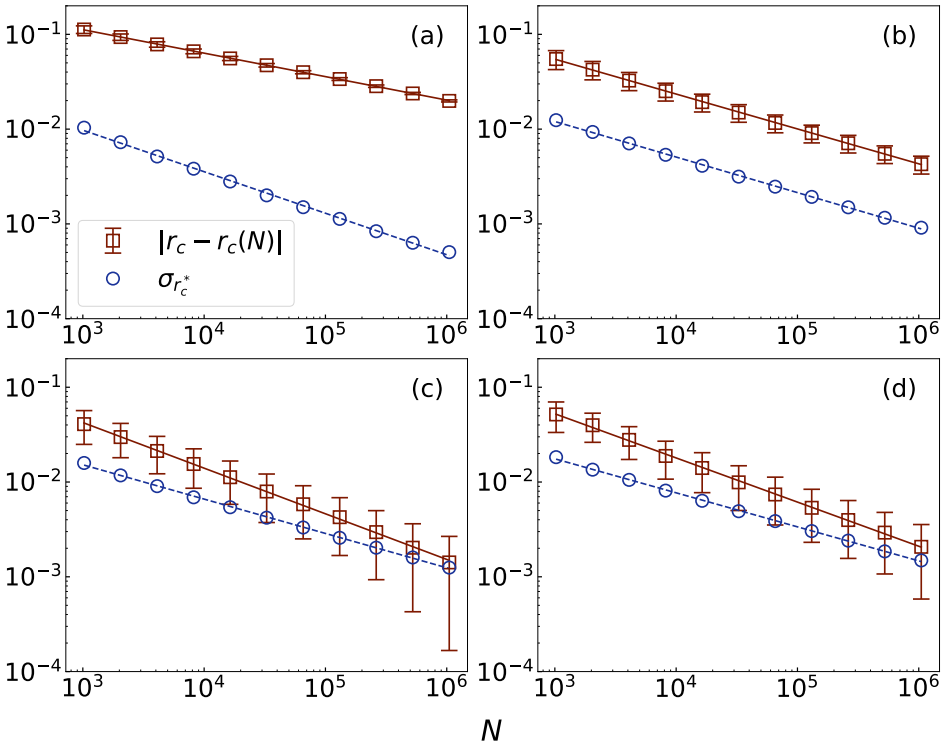

FIG. S6. **Estimation of $1/\bar{\nu}$.** Similar to Fig. 4 in the main, but results are valid for SPP with $C = 3$.

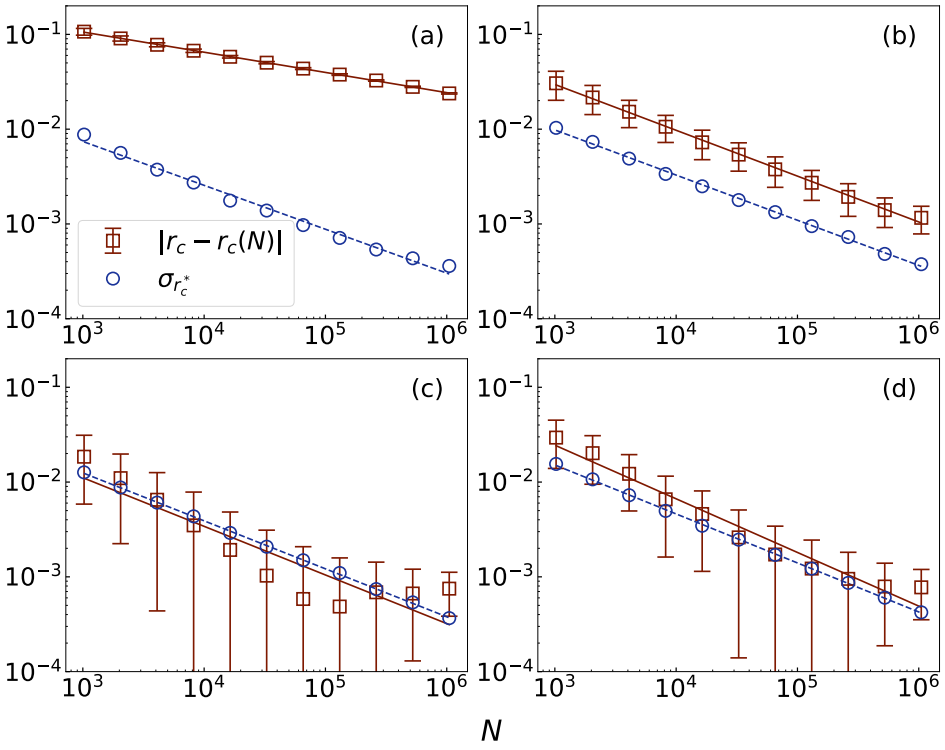

FIG. S7. **Estimation of $1/\bar{\nu}$.** Similar to Fig. 4 in the main, but results are valid for SPP with $C = N$.

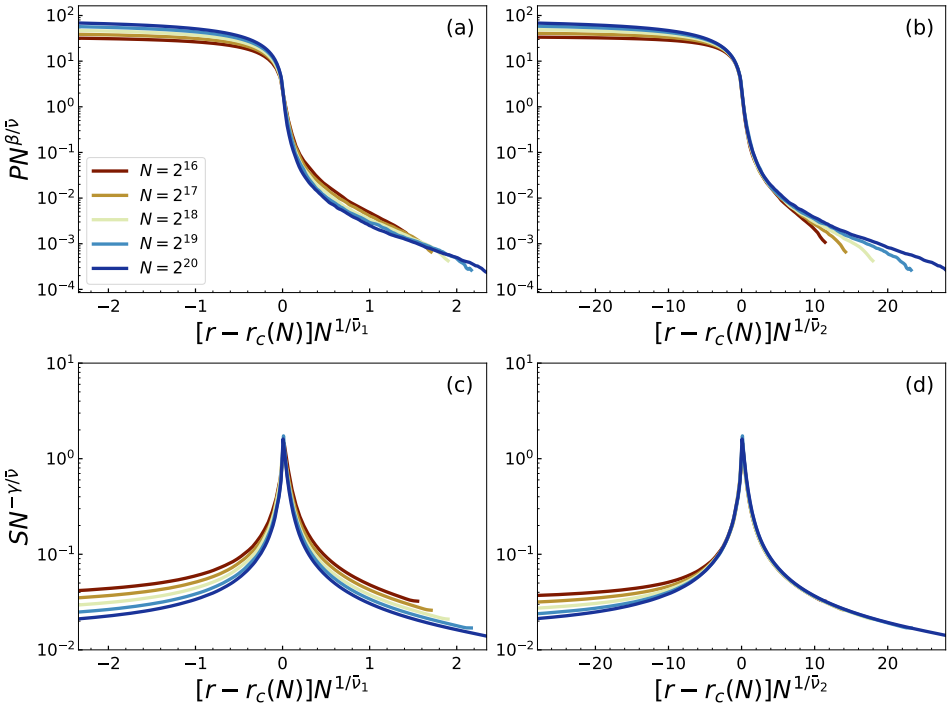

FIG. S8. **Data Collapse of P and S.** We plot the rescaled observable $PN^{\beta/\bar{\nu}}$ as a function of (a) $[r - r_c(N)]N^{1/\bar{\nu}_1}$ and (b) $[r - r_c(N)]N^{1/\bar{\nu}_2}$, respectively. Similarly, we plot the rescaled observable $SN^{-\gamma/\bar{\nu}}$ as a function of (c) $[r - r_c]N^{1/\bar{\nu}_1}$ and (d) $[r - r_c(N)]N^{1/\bar{\nu}_2}$, respectively. Results are valid for SFNs with $\lambda = 2.1$ and $k_{min} = 4$, and SPP model with $C = 2$. Note that in order to make a fair comparison between the data collapse using $1/\bar{\nu}_1$ and $1/\bar{\nu}_2$, the range of the abscissa is adjusted to display 200 bins of the curve for $N = 2^{20}$.

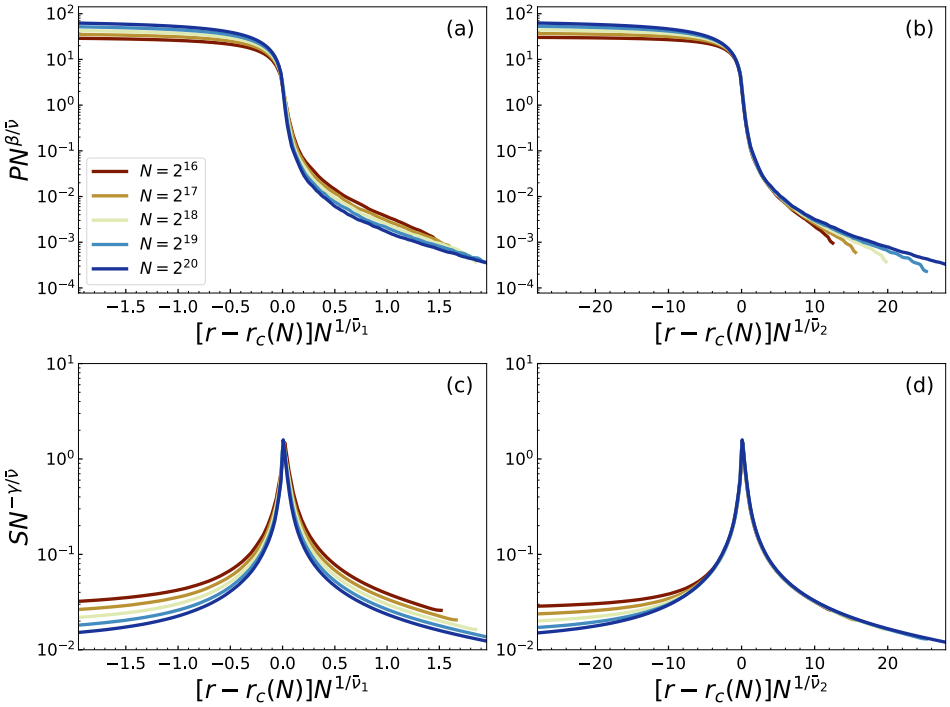

FIG. S9. **Data Collapse of P and S.** Similar to Fig. S8, but results are valid for SPP model with $C = 3$.

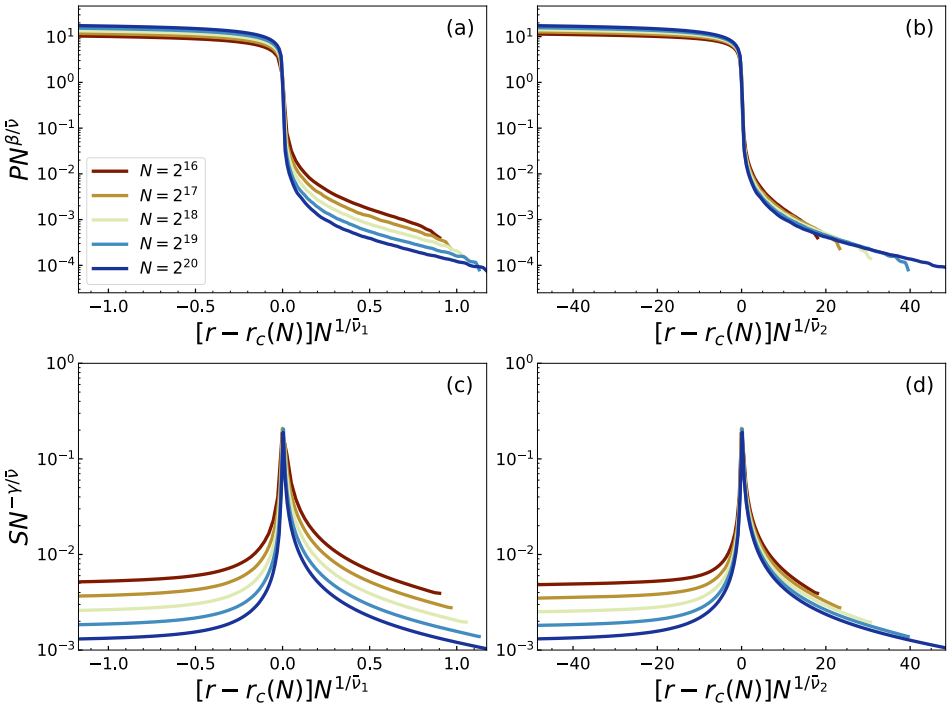

FIG. S10. **Data Collapse of P and S.** Similar to Fig. S8, but results are valid for SPP model with $C = N$.

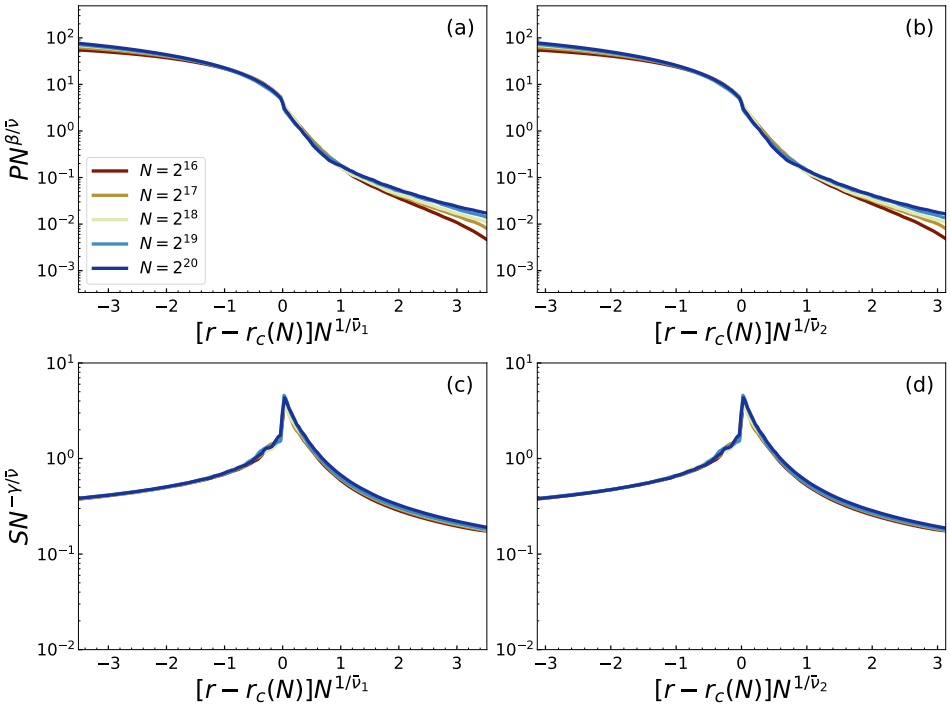

FIG. S11. **Data Collapse of P and S.** Similar to Fig. S8, but results are valid for SFNs with $\lambda = 3.5$ and $k_{min} = 4$, and SPP model with $C = 1$.

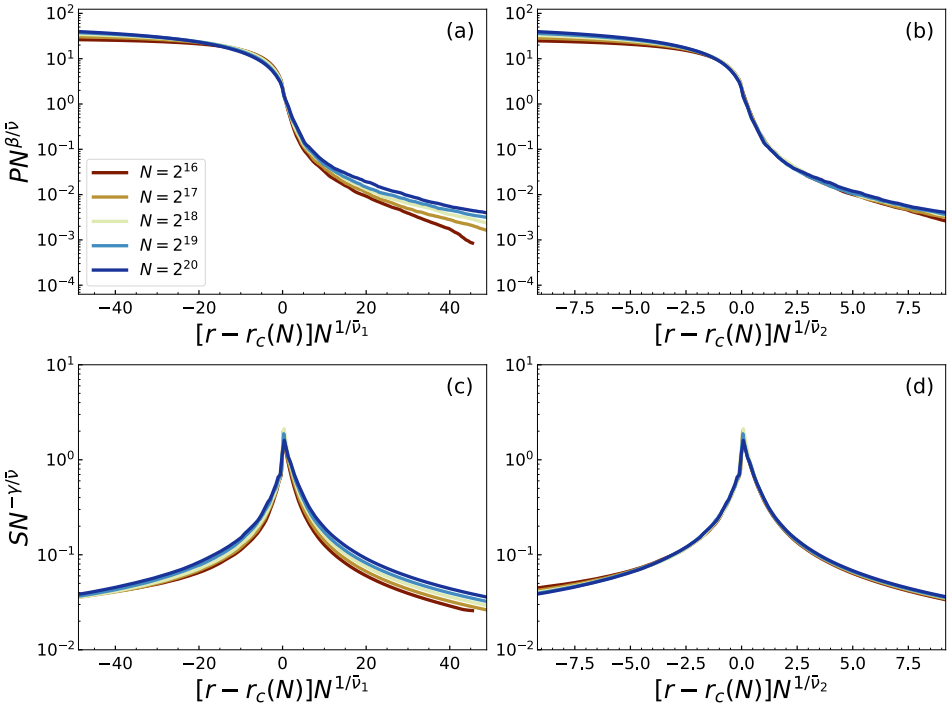

FIG. S12. **Data Collapse of P and S.** Similar to Fig. S11, but results are valid for SPP model with $C = 2$.

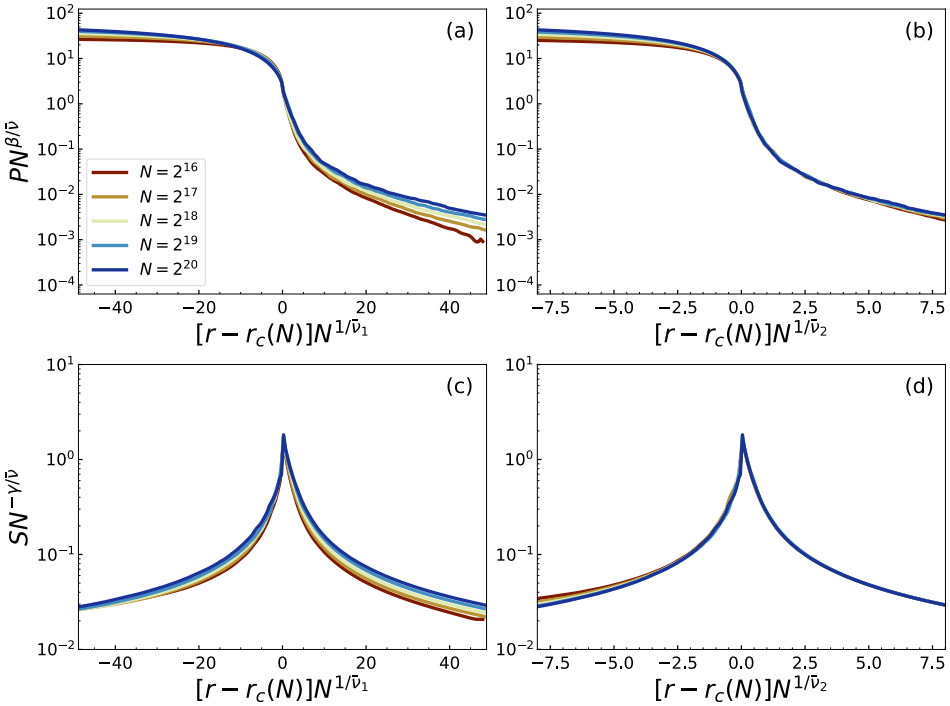

FIG. S13. **Data Collapse of P and S.** Similar to Fig. S11, but results are valid for SPP model with $C = 3$.

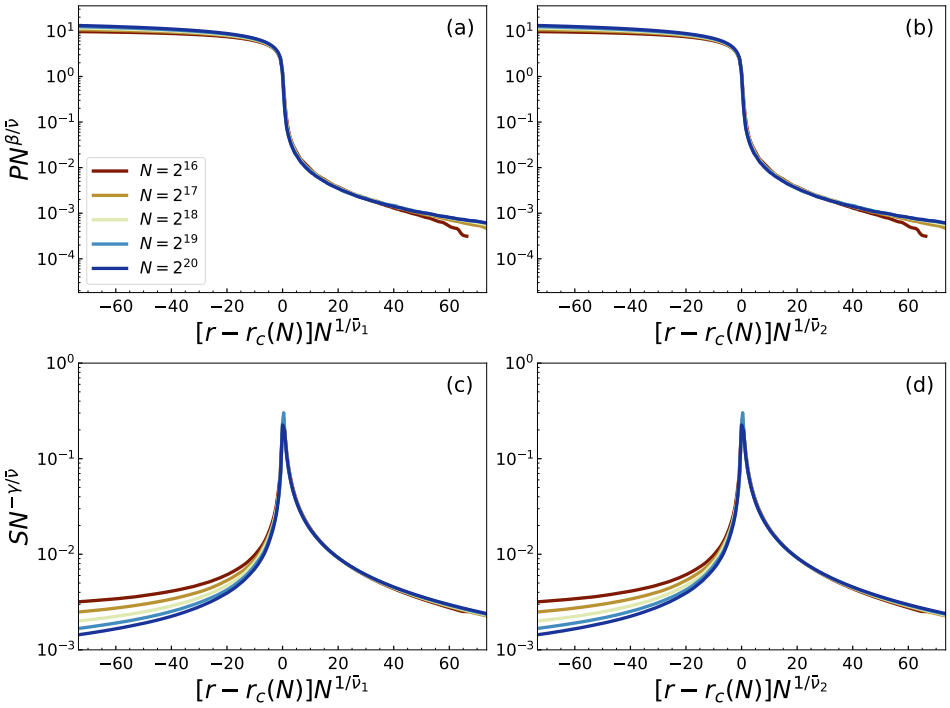

FIG. S14. **Data Collapse of P and S.** Similar to Fig. S11, but results are valid for SPP model with $C = N$.

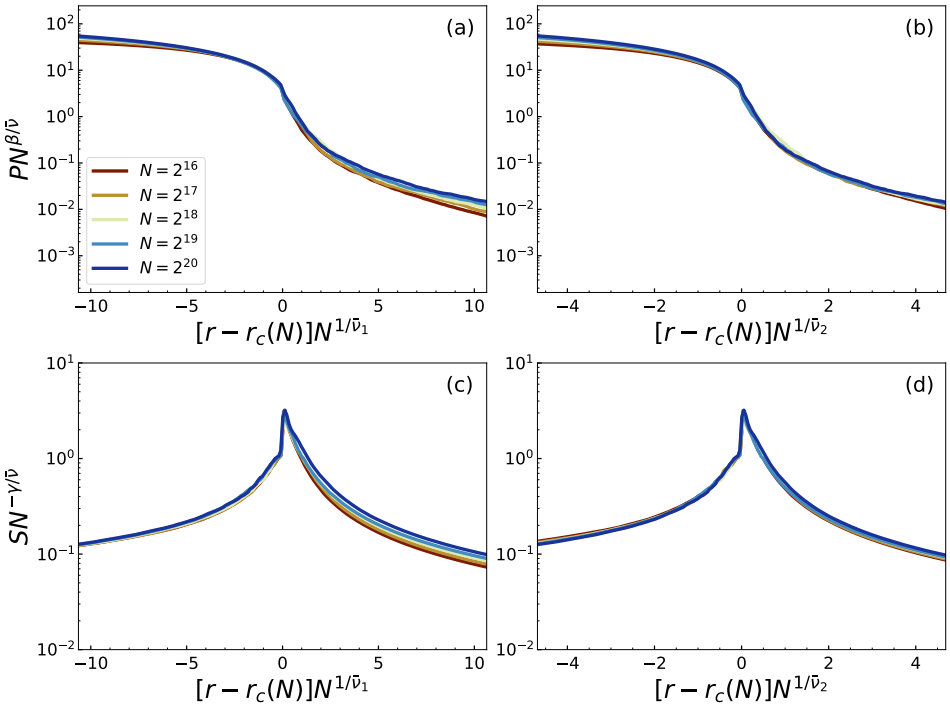

FIG. S15. **Data Collapse of P and S.** Similar to Fig. S8, but results are valid for SFNs with $\lambda = 4.5$ and $k_{min} = 4$, and SPP model with $C = 1$.

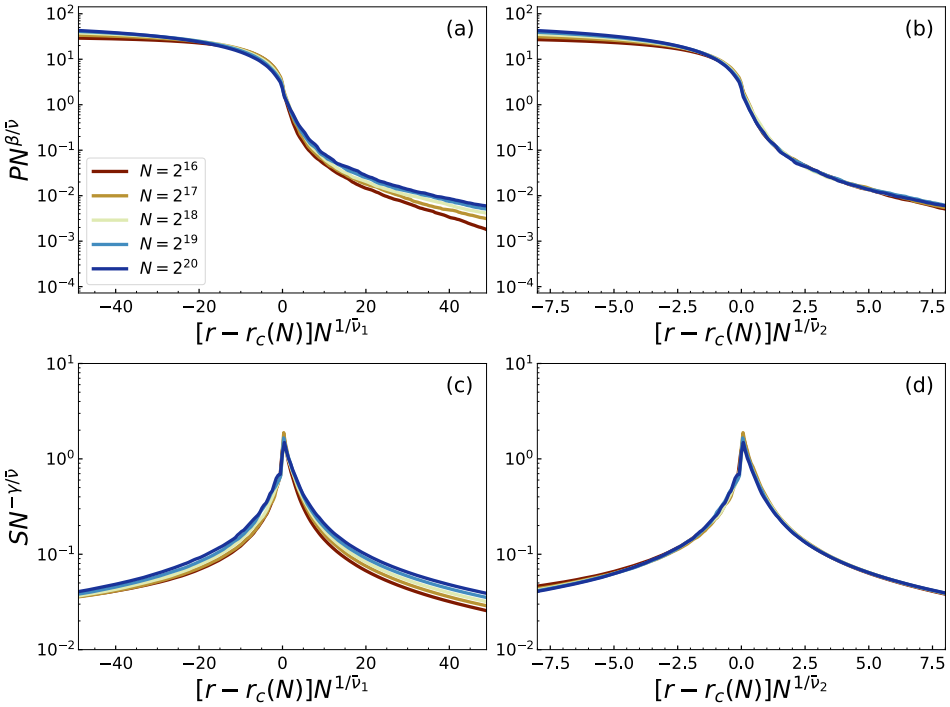

FIG. S16. **Data Collapse of P and S.** Similar to Fig. S15, but results are valid for SPP model with $C = 2$.

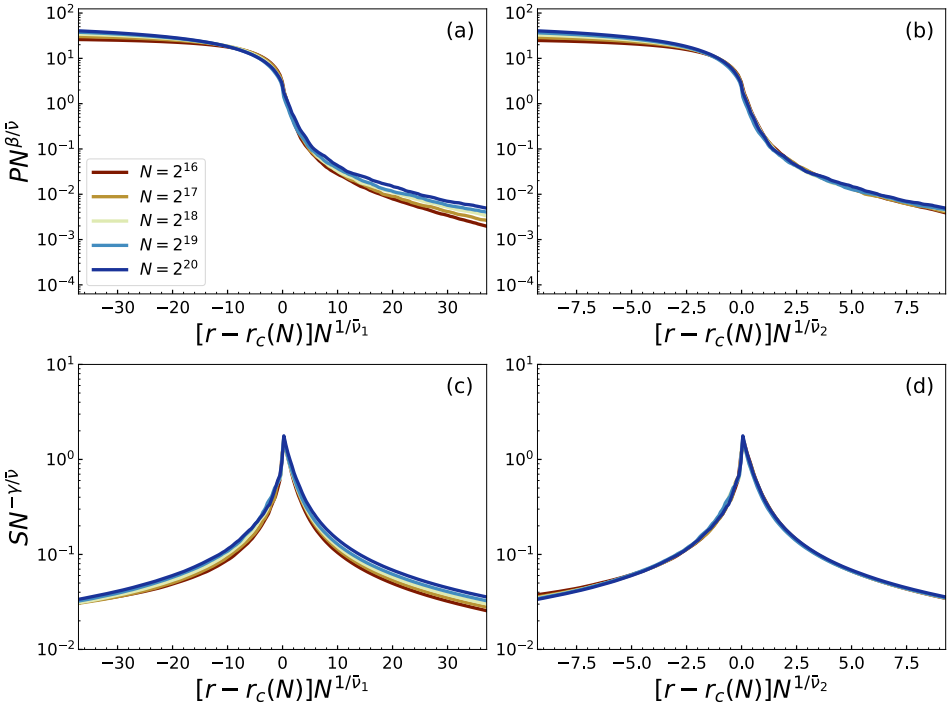

FIG. S17. **Data Collapse of P and S.** Similar to Fig. S15, but results are valid for SPP model with $C = 3$.

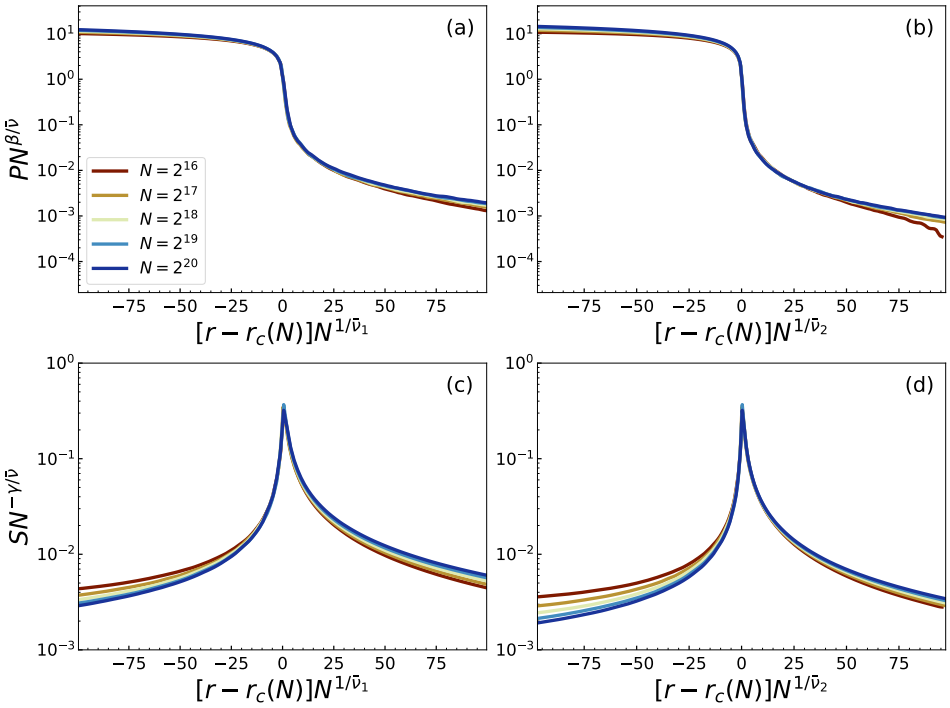

FIG. S18. **Data Collapse of P and S.** Similar to Fig. S15, but results are valid for SPP model with $C = N$.

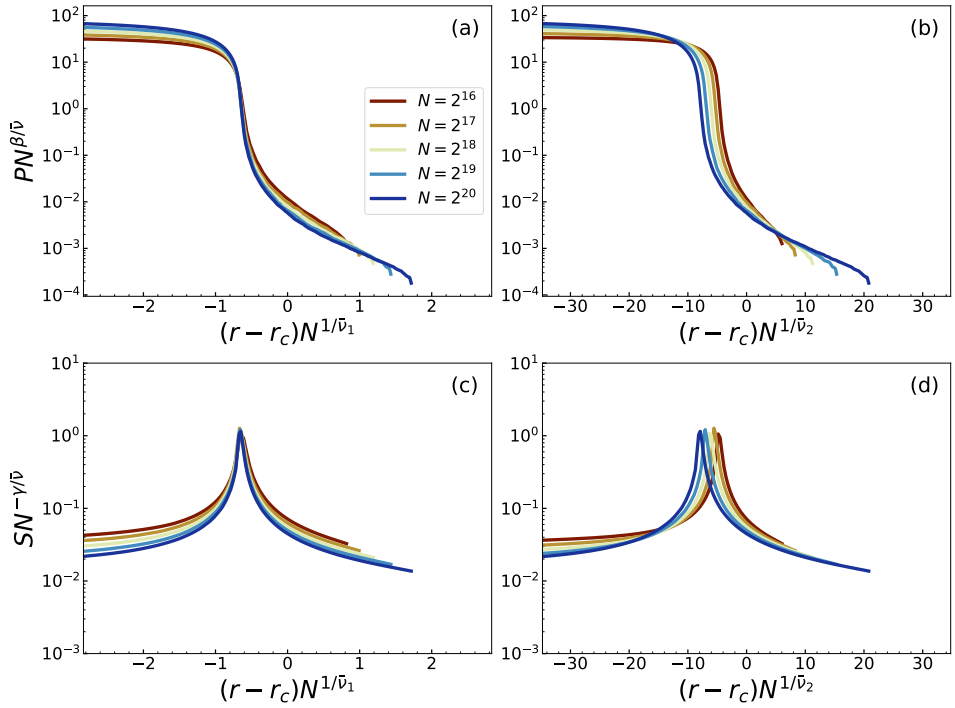

FIG. S19. **Data Collapse of P and S.** We plot the rescaled observable $PN^{\beta/\bar{\nu}}$ as a function of (a) $(r - r_c)N^{1/\bar{\nu}_1}$ and (b) $(r - r_c)N^{1/\bar{\nu}_2}$, respectively. Similarly, we plot the rescaled observable $SN^{-\gamma/\bar{\nu}}$ as a function of (c) $(r - r_c)N^{1/\bar{\nu}_1}$ and (d) $(r - r_c)N^{1/\bar{\nu}_2}$, respectively. Results are valid for SFNs with $\lambda = 2.1$ and $k_{min} = 4$, and SPP model with $C = 2$. Note that the range of the abscissa is adjusted to display 200 bins of the curves for $N = 2^{20}$.

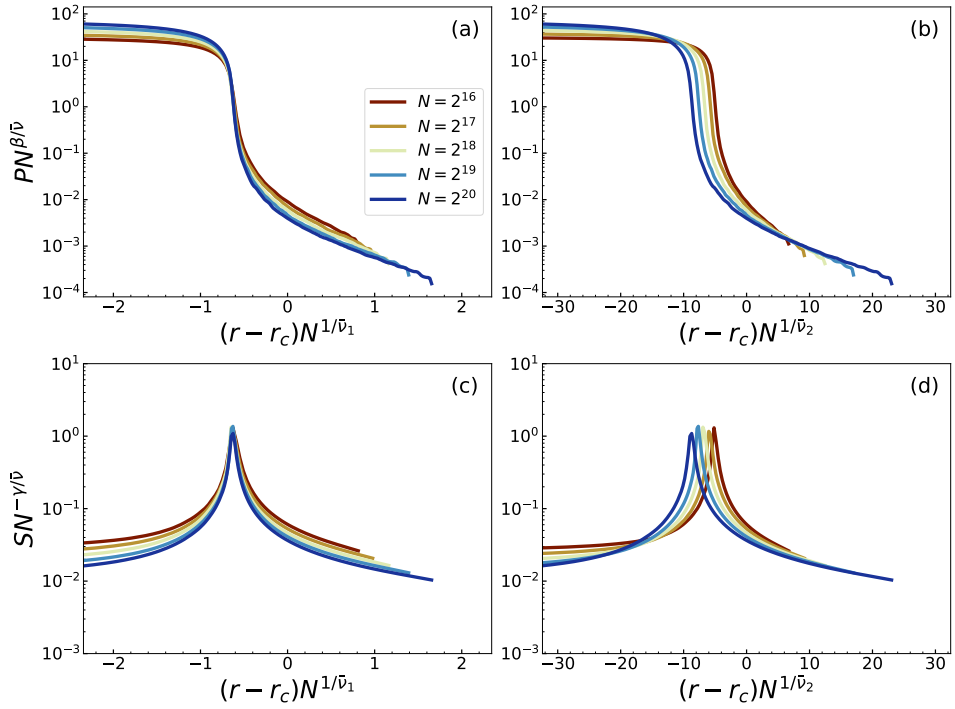

FIG. S20. **Data Collapse of P and S.** Similar to Fig. S19, but results are valid for SPP model with $C = 3$.

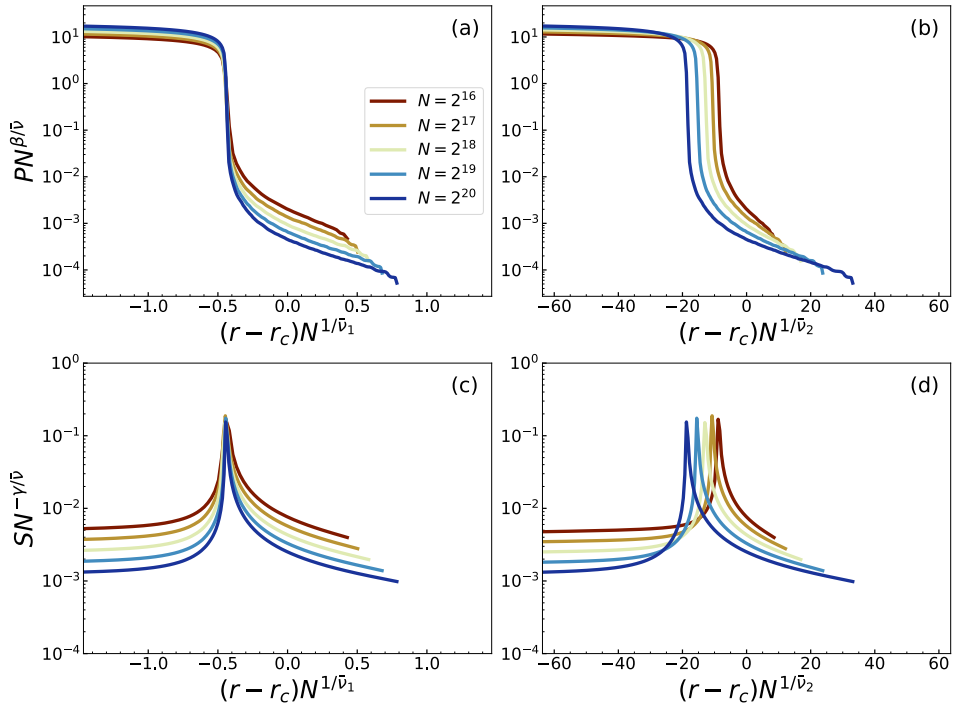

FIG. S21. **Data Collapse of P and S.** Similar to Fig. S19, but results are valid for SPP model with $C = N$.

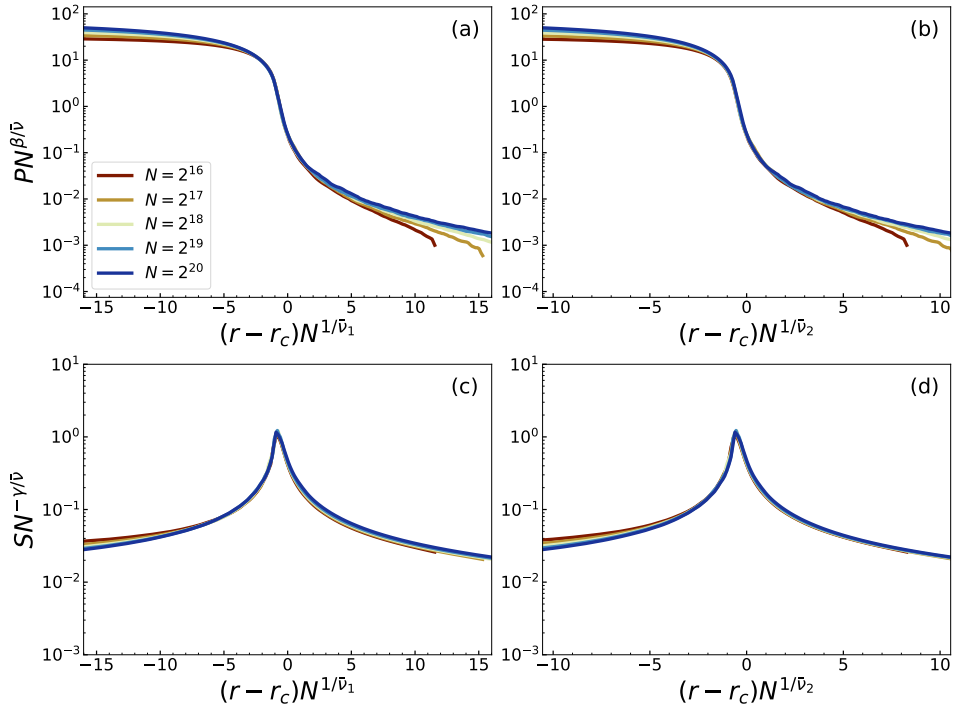

FIG. S22. **Data Collapse of P and S.** Similar to Fig. S19, but results are valid for SFNs with $\lambda = 2.7$ and $k_{min} = 4$, and SPP model with $C = 2$.

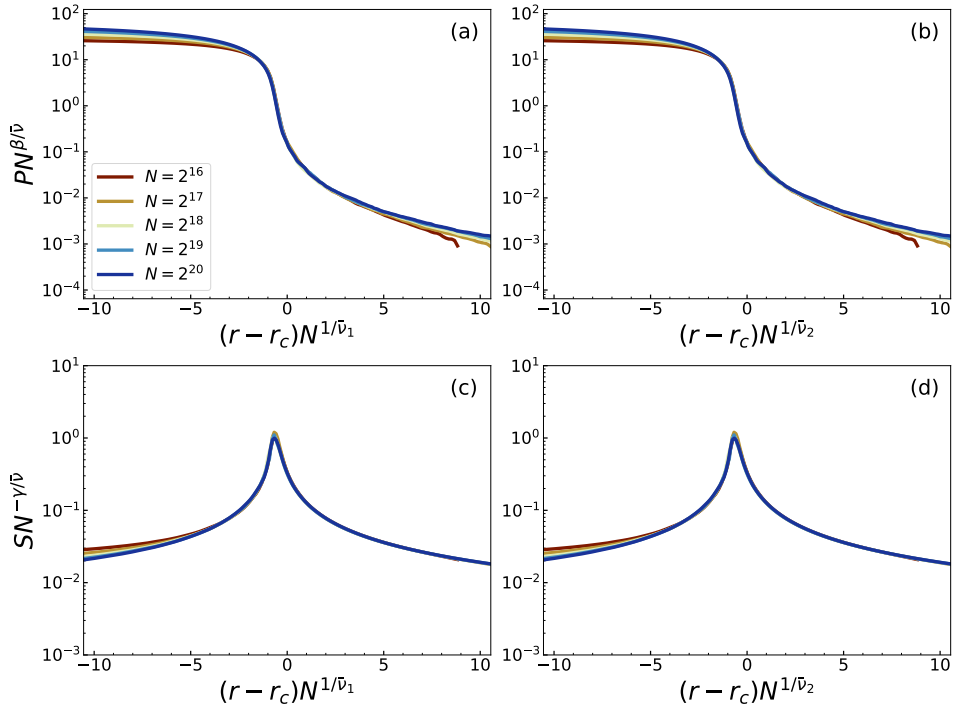

FIG. S23. **Data Collapse of P and S.** Similar to Fig. S22, but results are valid for SPP model with $C = 3$.

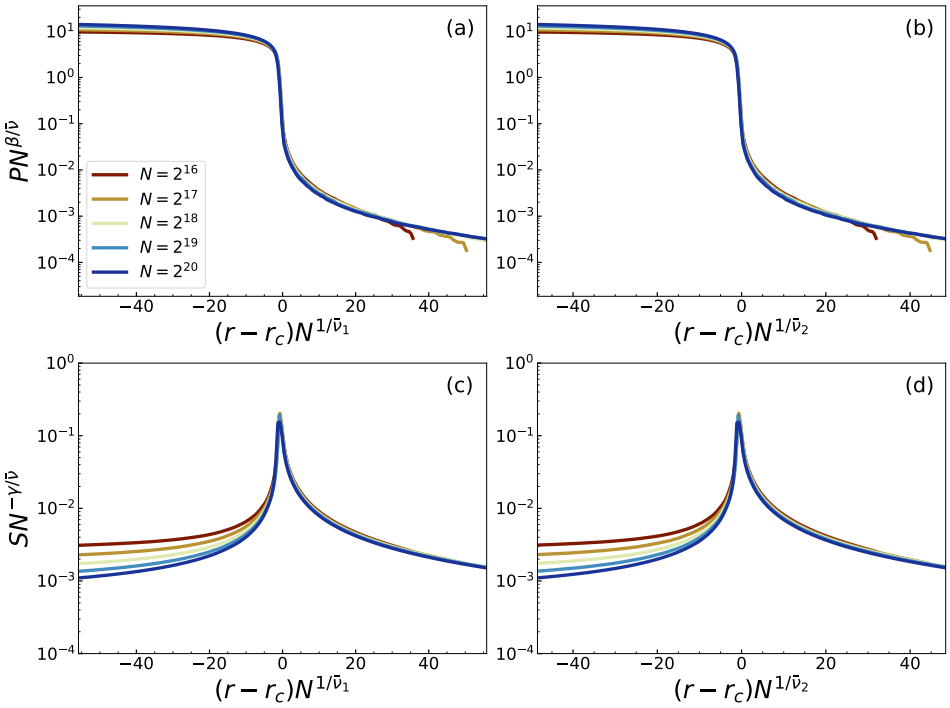

FIG. S24. **Data Collapse of P and S.** Similar to Fig. S22, but results are valid for SPP model with $C = N$.

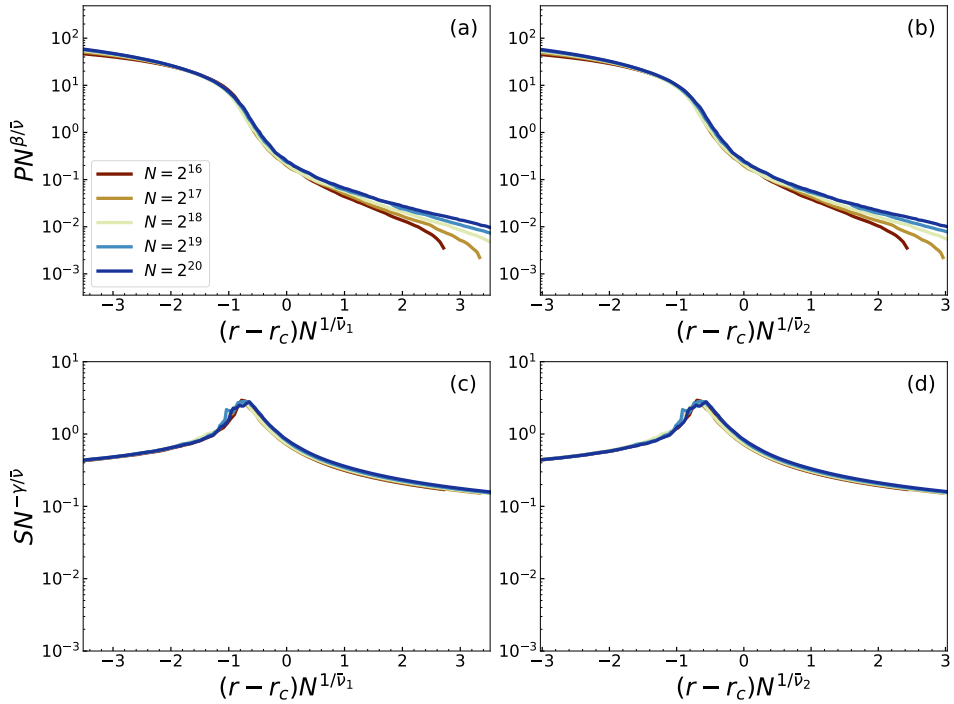

FIG. S25. **Data Collapse of P and S.** Similar to Fig. S19, but results are valid for SFNs with $\lambda = 3.5$ and $k_{min} = 4$, and SPP model with $C = 1$.

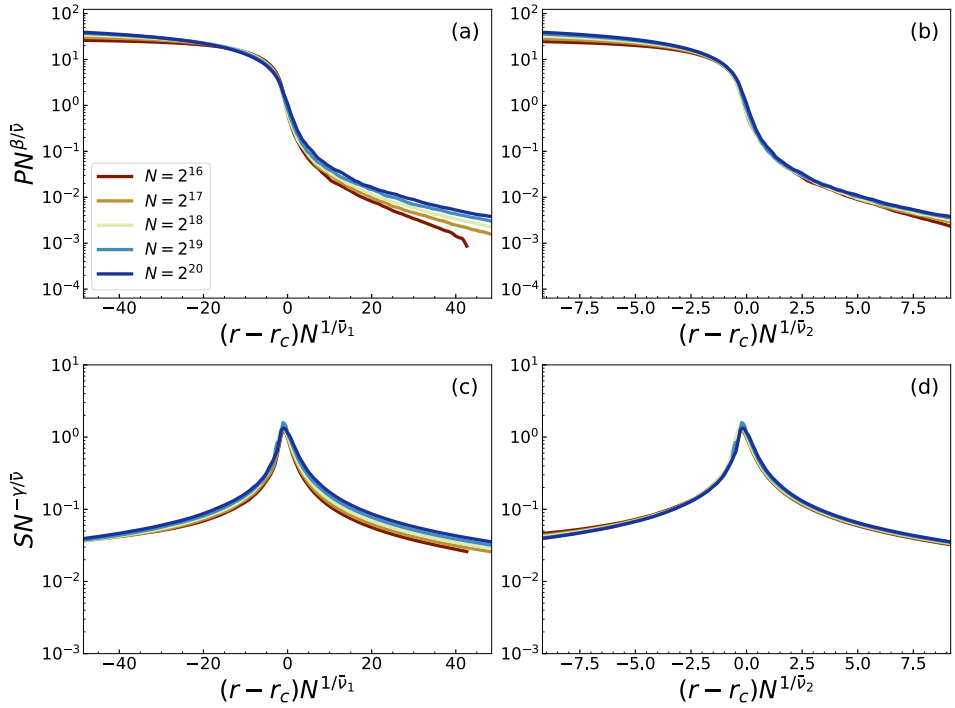

FIG. S26. **Data Collapse of P and S.** Similar to Fig. S25, but results are valid for SPP model with $C = 2$.

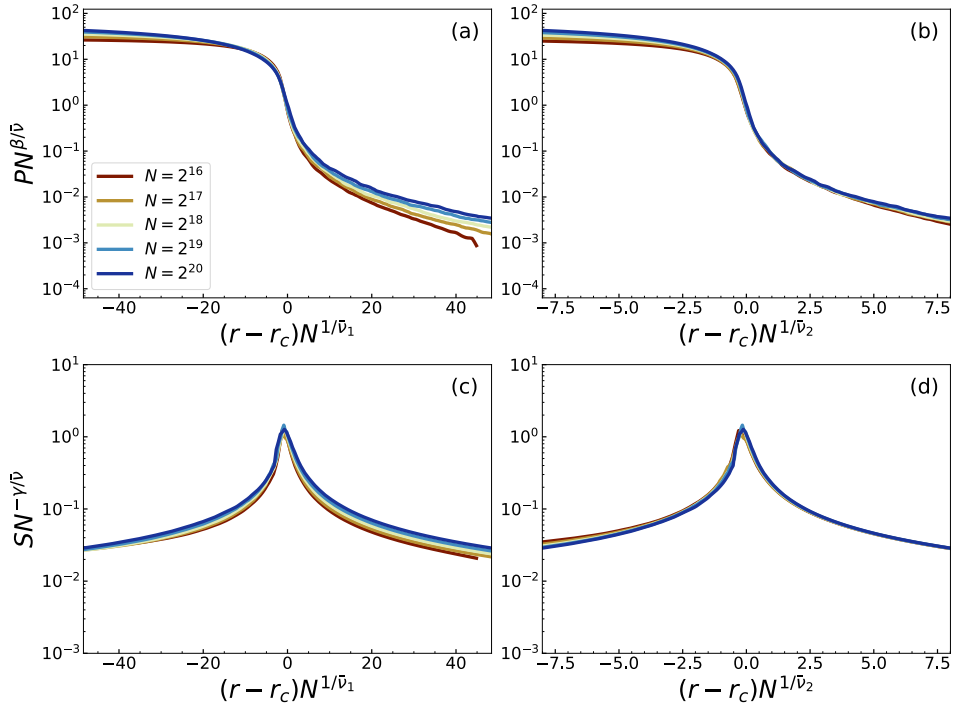

FIG. S27. **Data Collapse of P and S.** Similar to Fig. S25, but results are valid for SPP model with $C = 3$.

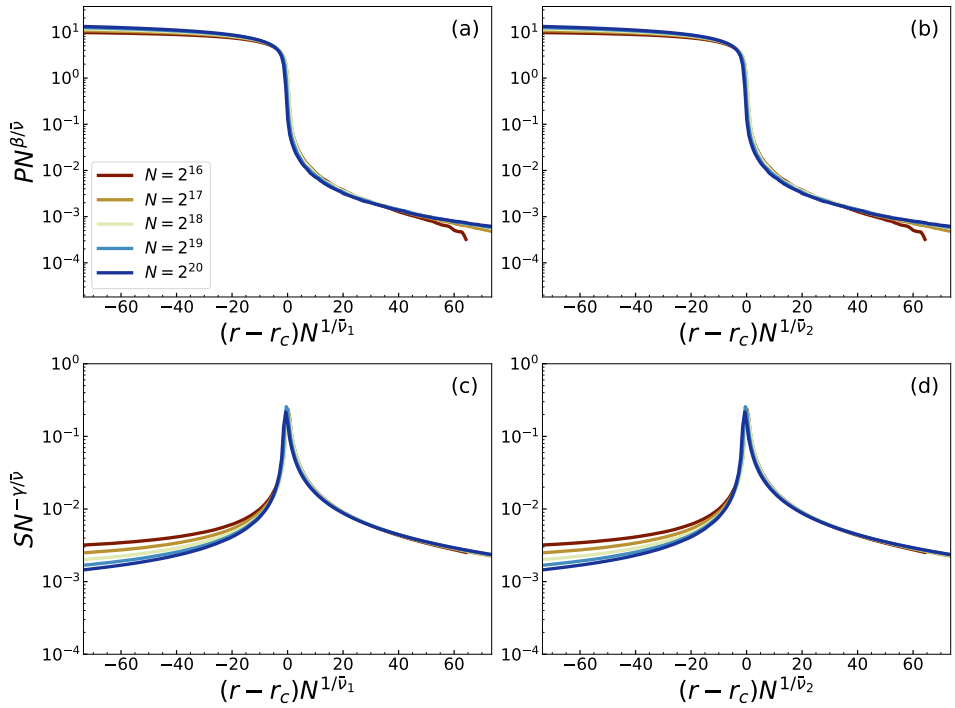

FIG. S28. **Data Collapse of P and S.** Similar to Fig. S25, but results are valid for SPP model with $C = N$.

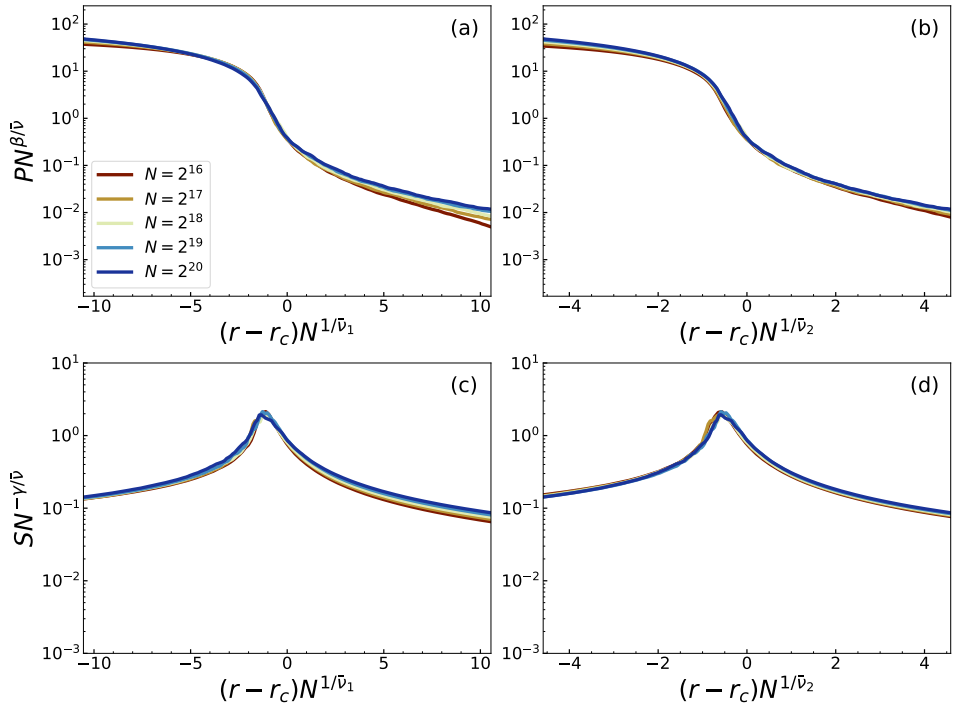

FIG. S29. **Data Collapse of P and S.** Similar to Fig. S19, but results are valid for SFNs with $\lambda = 4.5$ and $k_{min} = 4$, and SPP model with $C = 1$.

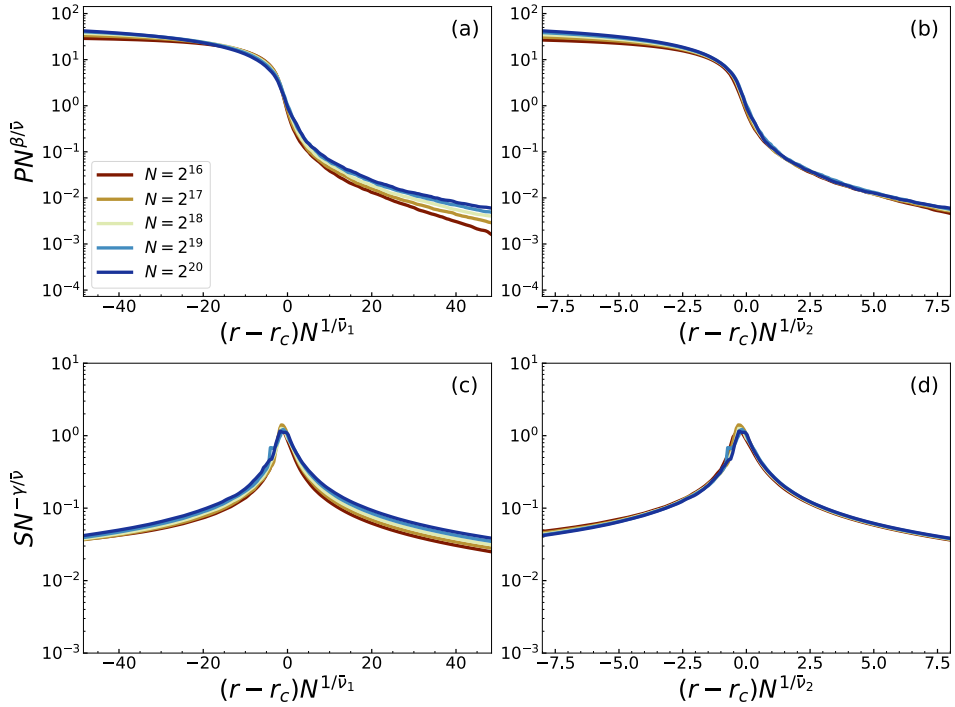

FIG. S30. **Data Collapse of P and S.** Similar to Fig. S29, but results are valid for SPP model with $C = 2$.

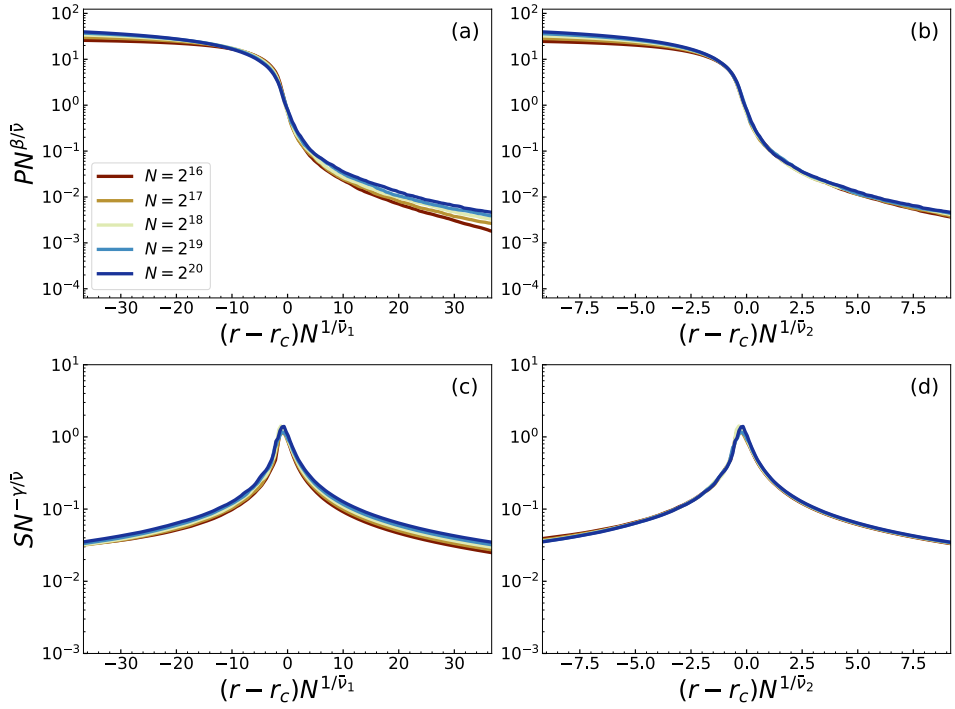

FIG. S31. **Data Collapse of P and S.** Similar to Fig. S29, but results are valid for SPP model with $C = 3$.

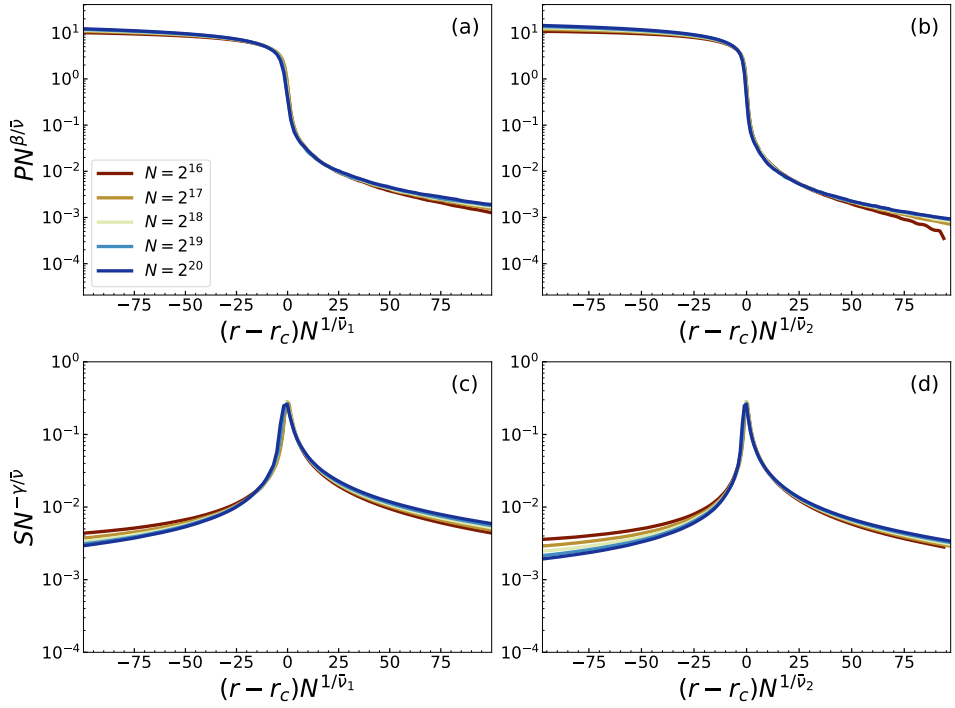

FIG. S32. **Data Collapse of P and S.** Similar to Fig. S29, but results are valid for SPP model with $C = N$.

SUPPLEMENTARY TABLES

In this section, we report detailed information related to the numerical simulations performed in this study.

λ	C	N	# of realizations
2.1	1	2^{10}–2^{20}	4000
	2	2^{10}–2^{17}	4000
		2^{18}	3000
		2^{19}–2^{20}	1000
	3	2^{10}–2^{17}	4000
		2^{18}	2000
		2^{19}	800
		2^{20}	350
	N	2^{10}–2^{16}	4000
		2^{17}	3000
		2^{18}	1000
		2^{19}	800
		2^{20}	300
2.7	1	2^{10}–2^{20}	4000
	2	2^{10}–2^{18}	4000
		2^{19}–2^{20}	2000
	3	2^{10}–2^{18}	4000
		2^{19}–2^{20}	2000
	N	2^{10}–2^{16}	4000
		2^{17}–2^{18}	3000
		2^{19}	1000
		2^{20}	700
3.5	1	2^{10}–2^{20}	4000
	2	2^{10}–2^{18}	4000
		2^{19}–2^{20}	2000
	3	2^{10}–2^{18}	4000
		2^{19}–2^{20}	2000
	N	2^{10}–2^{18}	4000
		2^{19}–2^{20}	1000
4.5	1	2^{10}–2^{20}	4000
	2	2^{10}–2^{18}	4000
		2^{19}–2^{20}	2000
	3	2^{10}–2^{18}	4000
		2^{19}–2^{20}	2000
	N	2^{10}–2^{18}	4000
		2^{19}–2^{20}	1000

TABLE S1. **Number of realizations.** We report the number of realizations of the shortest-path percolation processes used to estimate the critical point and the ratios of critical exponents. For a given initial network configuration, we repeated at most 10 times of the shortest-path percolation process.

C	N	# of realizations
1	2^{10}–2^{18}	300
	2^{19}–2^{20}	100
2	2^{10}–2^{18}	300
	2^{19}–2^{20}	100
3	2^{10}–2^{17}	300
	2^{18}	250
	2^{19}	100
	2^{20}	50
N	2^{10}–2^{17}	300
	2^{18}	200
	2^{19}	100
	2^{20}	50

TABLE S2. **Number of realizations.** We report the number of realizations used in Fig. 3 in the main. For a given initial network configuration, we repeated at most 10 times of the shortest-path percolation process.

N	# of bins	# of realizations
2^{16}	400	80
2^{17}	800	40
2^{18}	800	40
2^{19}	1600	40
2^{20}	1600	40

TABLE S3. **Binning information.** We report the number of bins and the number of realizations used in Fig. 5 in the main. This also applies to the other similar figures in the Supplementary Material. We clearly note that the binning was performed to reduce the visual noise in the figure, not to obtain the critical point or the ratio of critical exponents.

q	C	$\Omega_{o,1}$	ξ_1	$\Omega_{o,2}$	ξ_2
0.7	1	0.889(1)	0.330(3)	0.884(1)	0.287(2)
	2	0.000(1)	0.209(4)	0.000(1)	0.198(5)
	3	0.000(1)	0.210(3)	0.000(1)	0.198(3)
	N	0.000(1)	0.190(2)	0.000(1)	0.178(3)
0.8	1	0.779(1)	0.327(2)	0.768(1)	0.275(2)
	2	0.000(1)	0.235(5)	0.000(1)	0.224(5)
	3	0.000(1)	0.236(4)	0.000(1)	0.223(4)
	N	0.000(1)	0.220(4)	0.000(1)	0.206(4)
0.9	1	0.560(1)	0.308(1)	0.535(1)	0.252(1)
	2	0.000(1)	0.251(6)	0.000(1)	0.247(6)
	3	0.000(1)	0.251(6)	0.000(1)	0.246(5)
	N	0.000(1)	0.244(6)	0.000(1)	0.236(5)

TABLE S4. **Scaling of the ρ ratios.** We report the estimated variables $\Omega_{o,1}$, $\Omega_{o,2}$, ξ_1, and ξ_2 using Eq. (A2).